1	Deciphering the Interplay of Sludge Age and Aeration on Reactor
2	Performance and Microbial Dynamics in High-Rate Contact
3	Stabilization
4	Leiyu He ^a , Bing Guo ^b , Siegfried E. Vlaeminck ^c and Meng Wang ^{a*}
5	a. Department of Energy and Mineral Engineering and EMS Energy Institute, The Pennsylvania
6	State University, University Park, PA 16802, USA
7	b. Centre for Environmental Health and Engineering, School of Sustainability, Civil and
8	Environmental Engineering, University of Surrey, Surrey, GU2 7XH, United Kingdom
9	c. Research Group of Sustainable Energy, Air and Water Technology, Department of Bioscience
10	Engineering, University of Antwerp, Groenenborgerlaan 171, 2020 Antwerp, Belgium
11	* Corresponding author: 120 Hosler Bldg. The Pennsylvania State University, University Park, PA
12	16802, <u>mxw1118@psu.edu</u>
13	
14	

17

18

19

20

21

22

23

24

25

26

27

28

29

30

31

Abstract

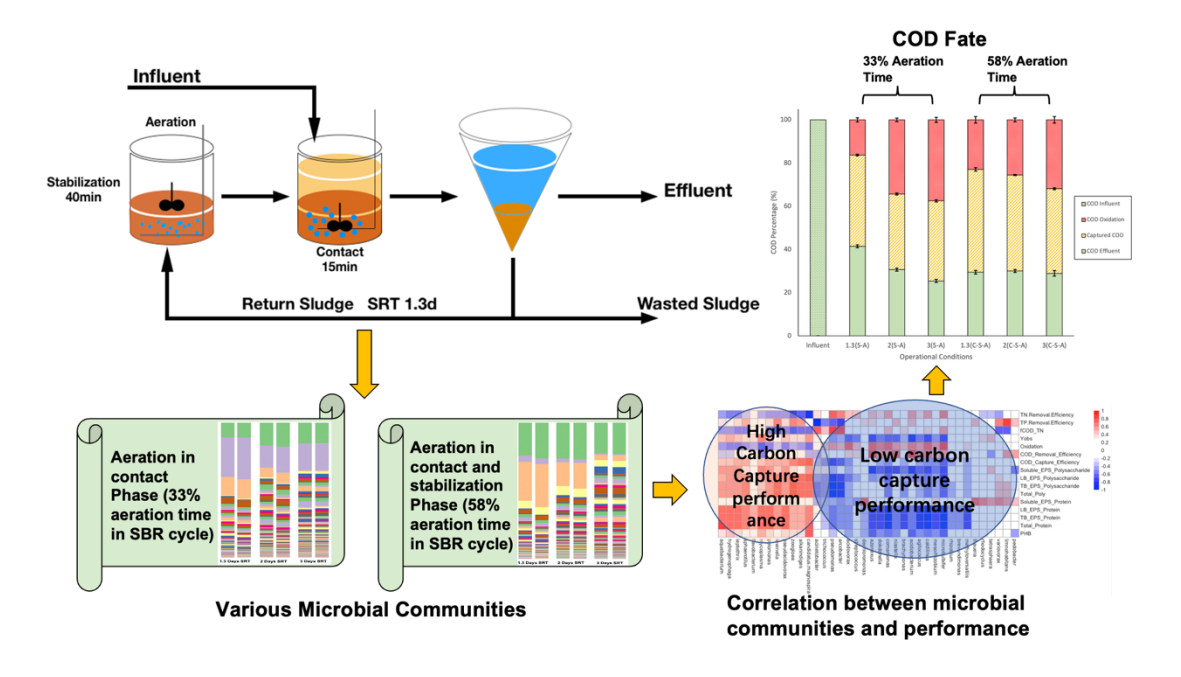
Redirecting wastewater organics from conventional energy-consuming aerobic biological removal to an energy-producing process can transform wastewater treatment plants into energy-neutral or energy-positive resource recovery facilities. This study explores the influence of solids retention times (SRTs) and the absence or presence of aeration in the contact phase on the reactor performance and the microbial community in high-rate contact stabilization (HiCS) reactors. Through high-throughput sequencing, we unveil the diversity and complexity of these microbial communities, pinpointing Aquabacterium and Acinetobacter as dominant species particularly susceptible to these parameters. The shifts in microbial communities had clear correlations with reactor performance, impacting carbon capture efficiency, total chemical oxygen demand removal, extracellular polymeric substances and polyhydroxyalkanoates production. SRT of 1.3 days with aeration in the contact phase resulted in significantly higher carbon capture efficiency. This work elucidates the intricate interplay between HiCS reactor settings, microbial dynamics and process performance, paving the road for future work optimizing operational conditions in scaled HiCS reactors.

32

33

- Key Words: Wastewater carbon Redirection; High-Rate Activated Sludge; Microbial
- 34 Ecology; EPS; PHA

36 Graphical Abstract



40

41

42

43

44

45

46

47

48

49

50

51

52

53

54

55

56

57

58

59

1. Introduction

The growing global wastewater treatment demand and more stringent nutrient discharge limits increase the energy consumption of wastewater treatment plants (WWTPs). Water and wastewater treatment accounts for approximately 2% of national electricity usage in the United States. 1 Wastewater treatment typically consumes around 0.75 kWhe/m³, whereas extractable energy from wastewater is around 2.72 kWh_e/m³, which can be harvested to offset the high energy demand. ² Redirecting wastewater organic carbon from aerobic oxidation and respiration to energy production is necessary to transform WWTPs to energy-neutral or even energy-positive resource recovery facilities. ³ Energy consumption can be further reduced by combining carbon capture with alternative nitrogen removal processes, for instance based on anammox. Chemically enhanced primary treatment (CEPT) and high-rate activated sludge systems (HRAS) can be integrated into existing infrastructure for carbon capture. 4 Although CEPT has a high hydraulic throughput and can remove 45-85% of total chemical oxygen demand (COD), it is not efficient in removing soluble COD (sCOD). ⁵ HRAS is characterized by the high loading rate (>2 kg COD VSS ⁻¹ day ⁻¹) and short solids residence time (SRT) (< 2 days), which can achieve carbon removal efficiencies of 50-75% and carbon harvesting efficiencies of 24-55%. ⁶ Both particulate COD (pCOD) and sCOD can be removed by HRAS. ^{7,8} The high-rate contact stabilization (HiCS) process is one variant of HRAS that aims to improve biosorption and storage phenomena by creating a feast-famine regime. 4 Biosorption occurs on the surface of

the cell membrane, where organic matter is adsorbed by extracellular polymeric substances (EPS), 9 which can subsequently be transformed to intercellular storage compounds, such as polyhydroxyalkanoates (PHA) and glycogen. 10 In the HiCS, influent with organic compounds flows into the contact tank to create a feast condition; after settling and decanting, the mixed liquor sludge returns into the stabilization tank with aeration to create a famine condition. The rapid shifts between feast and famine conditions, typically lasting less than an hour, select microorganisms that can store excess substrates and nutrients in cells quickly as a survival strategy. ¹¹ Other carbon capture process, such as coagulation-enhanced high-rate contact stabilization process, achieved up to 60% carbon capture efficiency and 30-40% phosphorus removal. ¹² The combination of HRAS systems with anaerobic membrane bioreactors (AnMBR) is another feasible technology, ¹³ where the COD capture efficiency of HRAS was as high as 43%, and the total COD recovery in the form of methane in AnMBR reached 30%. An automated pilot-scale HiCS system, which used real-time responses to control oxygen uptake rate (OUR) ratio between the contact and stabilization tanks, has been investigated to improve the carbon capture efficiencies. 14

60

61

62

63

64

65

66

67

68

69

70

71

72

73

74

75

76

77

78

79

80

81

Operational parameters such as dissolved oxygen (DO) and SRT play a critical role in organic carbon capture efficiency. In HRAS systems, Kinyua et al. found that the concentrations of EPS proteins and polysaccharides were proportional to DO under low SRT (0.28 day) conditions. ¹⁵ In addition, storage compounds such as PHA also increased with increasing DO concentration. Low DO concentration in activated sludge systems leads to slower microbial metabolic activity and growth, which may reduce the

production of EPS and PHA. ^{16,17} However, the impact of the operational conditions in the contact and stabilization tanks on EPS production within HiCS systems remains a contentious issue in the literature. Famine conditions in the stabilization tank were found to induce EPS production of the sludge. ¹⁸ Further, prior research observed higher EPS concentrations in the contactor, suggesting this step plays a crucial role in improving bioflocculation. ^{4,19} Despite these findings, the mechanisms of EPS production and content in response to operation conditions and carbon harvesting efficiency in HiCS systems still need further investigation.

Microbial communities in bioreactors determine the functions and stability of the process. The complexity and dynamics of these microbiomes, however, lead to great challenges to describing the ecology of engineered systems. In the HiCS procnitriess with low SRT and short contact/stabilization cycles, microbial communities are different from those in conventional activated sludge systems. The traditional niche theory assumes that changes in microbial communities can be predicted based on defined environmental conditions. ²⁰ Changes in operational conditions may lead to different dominant genera. ^{17,21,22} The ecological function may be predicted if there is sufficient information on the operational conditions. Therefore, understanding the relationship between operational parameters, reactor performance, and microbial communities is crucial to elucidate the mechanism of carbon capture in HiCS and provide a theoretical basis for large-scale applications.

Previous studies on HiCS compared the effects of different contact and stabilization times, aeration conditions, and sludge ages on the reactor performance^{4,23}.

However, limited understanding exists regarding the impact of operation conditions on the dynamics of the microbial community, the metabolism pathways of carbon storage in the form of PHA and the relationship between microbial community composition and reactor performance. The objectives of this research are to: 1) evaluate the impact of SRT and aeration conditions on the fate of organics in the HiCS process; 2) investigate the relative contributions of storage of organic matters by EPS and PHA content; 3) explore the dynamics and functions of the microbial communities in HiCS under different operational conditions.

2. Method

2.1 Operation of the reactors

Duplicate 4L lab-scale reactors were operated in sequencing batch mode to mimic the HiCS process. The operation sequence of each cycle is shown in Fig. 1. Contact time of 15 minutes and stabilization time of 40 minutes were selected in this study. ²⁴ The reactors were inoculated with 1:1 (v/v ratio) mixture of activated sludge from the aeration and the anoxic tanks of a local wastewater treatment plant (State College, PA). The reactors were fed with 25% (v/v) of primary effluent and 75% (v/v) of synthetic wastewater to keep total COD (tCOD) around 400 mg/L. ²⁵ The composition of synthetic wastewater is shown in Table S3. Samples of the mixed influent were collected daily for COD analysis. The hydraulic retention time (HRT) of the reactors was 4 hours. Both reactors were operated in a 20°C constant temperature room. Different aeration conditions and SRTs were applied in six stages of operation (Table

1). The SRT was determined as the ratio of the mass of activated sludge in the reactor to the mass of sludge leaving the system through sludge wasting and effluent decanting (Eq.1). The biomass concentrations during the contact and decanting phases were used in the calculation for the ease of reactor operation. DO was controlled by intermittent aeration at 1 min on and 3 min off based on a preliminary experiment. Two aeration conditions were evaluated in this study: (i) absence of contact-phase aeration, and hence aeration provided in stabilization phase only, named S-A, yielding 33% aeration time in one SBR cycle, versus (ii) aeration in both contact and stabilization phases, named C-S-A, yielding 58% aeration time in one SBR cycle. The aerobic SRT (AerSRT) is determined by multiplying SRT with the percentage of aeration time. ²⁶ Extended aeration at the contact phase was included in this study to provide an in-depth understanding of the impact of aeration on the dynamics of microbial community in HiCS reactors.

139
$$SRT = \frac{X_{VSS,activated sludge} \times V_{contact}}{X_{VSS,waste} \times Q_{waste} + X_{VSS,effluent} \times Q_{effluent}} \qquad Eq. 1$$

Where, X_{VSS} is the VSS concentrations of the wasted sludge, effluent or activated sludge in contact phase; V is the volume of mixed liquor in contact phase; Q is the flow rate of wasted sludge or effluent.

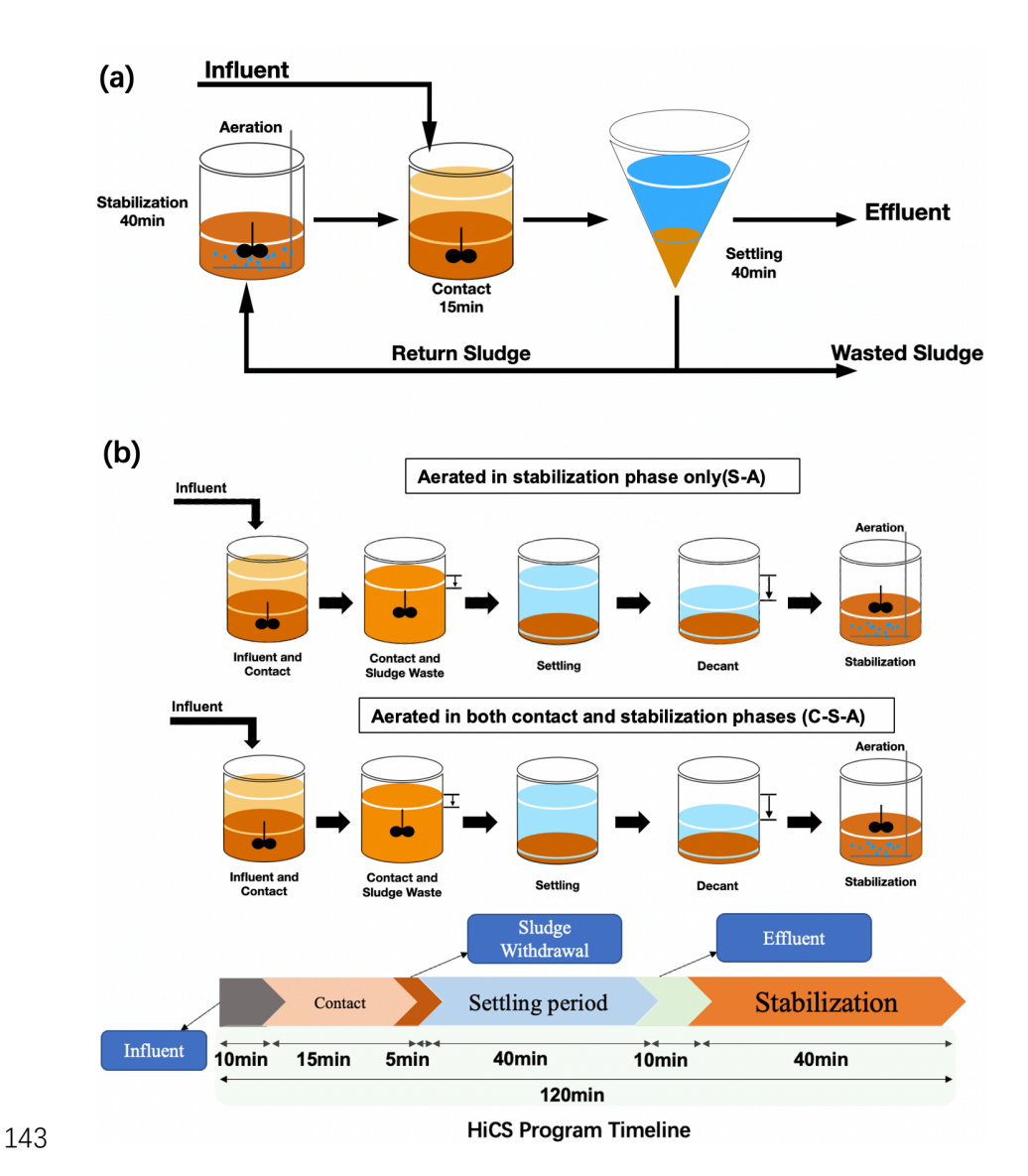


Fig. 1. Set up of HiCS process. (a). Schematic of HiCS process design; (b). Sequencing batch reactors (SBR) mimicking the HiCS process and operational steps in a combined one-reactor and settler system in this study.

Table 1. Operation conditions of HiCS reactors. (C-S-A: Aerated in both contact and stabilization phase; S-A: Aerated in stabilization phase only)

Stages	Aeration conditions	SRT (Days)	DO in Contact Phase (mg/L)	DO in Stabilization Phase (mg/L)	Operational Periods (Days)
Stage 1		3	0	2-3	0-14
Stage 2	Stabilization Aeration (S-A)	2	0	2-3	15-25
Stage 3		1.3	0	2-3	26-42
Stage 4		3	1-2	2-3	43-57
Stage 5	Contact- Stabilization- Aeration (C-S-A)	2	1-2	2-3	58-68
Stage 6	11010000 (0 5 11)	1.3	1-2	2-3	69-84

2.2 EPS extraction and analysis

A modified heating extraction method was used for EPS extraction. ²⁷ Briefly, 50 mL mixed liquor samples were collected at the end of the contact phase and centrifuged at 6000g for 5 min. The supernatant was collected as soluble EPS (S-EPS). The pellet was then resuspended into 20 mL of 25% diluted Ringer's solution that had been preheated to 60°C. After vortexing for 1 min, the sample was centrifugated at 6000g for 10 min and the supernatant was collected as the loosely-bound EPS (LB-EPS). The pellet was resuspended again using 20 mL diluted Ringer's solution and heated at 70°C for 30 min. The supernatant was collected after 6000g centrifugation for 15 min and was considered as tightly-bound EPS (TB-EPS). The protein concentrations of EPS were analyzed by the Lowry method using PierceTM Modified Lowry Protein Assay Kit (Thermo Fisher). ²⁸ The polysaccharide concentrations were measured by the phenol-sulfuric acid method. ²⁹

2.3 PHA extraction and analysis

Pellets after EPS extraction were stored at -20°C for future PHA extraction. ¹⁵ Stored samples were thawed and centrifuged at 4000g for 10 min to remove the supernatant and then dried at 100°C for 4 hours in the oven. 2 mL of chloroform and 2 mL of acidified methanol were added to the 10 mL centrifuge tube containing 20 mg of the dried EPS extracted pellet. The acidified methanol solution was prepared by adding 10 mL of 98% H₂SO₄ in 90 mL ethanol. The samples were incubated in an oven at 100°C for 3.5 h. After cooling to room temperature, 1 mL of chloroform and 2 mL of 14% aqueous ammonia solution were added. After completely mixing and standing for

5 min, 0.5 mL sample from the lower chloroform layer was transferred to a GC sampling bottle. The concentrations of three different types of PHAs, including polyhydroxybutyrate (PHB), polyhydroxyvalerate (PHV), and poly-β-hydroxy-2-methylvalerate (PH2MV), were measured by GC-FID equipped with a DB-Wax column (15 m, 0.53 mm ID, 1 μm film thickness).

2.4 Analytical methods

173

174

175

176

177

178

179

180

181

182

183

184

185

186

187

188

189

190

191

192

193

194

Influent, effluent, and sludge samples were collected daily for chemical analyses. Influent and effluent samples were filtered by 0.45 µm filter paper for sCOD, cation and anion analyses. Unfiltered samples were used for tCOD, total nitrogen (TN) and total phosphorus (TP) analysis. Particulate COD (pCOD) was obtained by subtracting sCOD from tCOD. The COD concentrations were analyzed by the VWR COD kit (BDH0403-150). Total suspended solids (TSS) and volatile suspended solids (VSS) measurements followed the 2540 standard method. ³⁰ DO, pH, and temperature were measured with probes (ORION STAR A216, Thermo Scientific). Ion Chromatography (DIONEX AQUINO, Thermo Scientific) was applied to determine the concentrations of Cl⁻, NO₂⁻, NO₃⁻, SO₄²-, PO₄³-, Na⁺, NH₄⁺, K⁺, Mg²⁺, and Ca²⁺. TN and TP were analyzed using Hach Test Kits TNT827 TNTplus and TNT826 TNTplus, respectively. The food-to-microorganism (F/M) ratio was calculated by dividing the amount of food (COD) per day by the amount of microorganisms (VSS) in reactors. The specific COD removal rates was calculated by dividing the amount of removed COD in HiCS process per day by the amount of VSS in reactors (Eq. 2). The product of XVSS and Vreactor represents the total mass of VSS in the reactor.

Specific COD removal rates =
$$\frac{COD_{effluent} \times V_{effluent}/day}{X_{VSS,activated sludge} \times V_{reactor}}$$
 Eq. 2

197

2.5 Determination of the COD balance and observed yield

- The COD balance including COD capture and oxidation efficiencies were
- determined by COD in influent, effluent and wasted sludge (Eq. 3-6). Average values
- in each operational stage were used in the calculation.

$$COD_{input} = COD_{influent} \times V_{influent} / day \qquad Eq. 3$$

$$202 \quad COD_{output} = COD_{effluent} \times V_{effluent}/day + X_w \times f_{COD}/_{TSS} \times V_{effluent}/day \ Eq. \ 4$$

$$COD_{captured} = X_w \times f_{COD/_{VSS}} \times \frac{V_{effluent}}{day}$$
 Eq. 5

$$COD_{oxidation} = COD_{input} - COD_{output}$$
 Eq. 6

- Where, COD_{influent} and COD_{effluent} are tCOD concentrations of the influent and the
- effluent, respectively; COD_{output} is the tCOD in the effluent and wasted sludge; X_w is
- the VSS concentrations of the wasted sludge; V_R is the volume of the reactor;
- 208 $f_{COD/_{VSS}}$ is the experimentally obtained conversion factor of VSS to tCOD. The
- 209 loss of COD was considered as aerobic oxidation to CO₂.
- 210 The observed growth yield (Y_{obs}) represented the ratio of biomass production to
- 211 the mass of organic matter consumed in the HiCS process. The observed yield (Y_{obs})
- 212 was calculated following modified methods by prior research, ³¹ as shown in Eq.7 and
- 213 Eq.8.

214
$$\Delta X_{growth}({^{gVSS}/_{day}}) = X_{VSS,waste} \times V_{waste} + X_{VSS,effluent} \times V_{effluent} \qquad Eq. 7$$

215
$$Y_{obs} = \frac{\Delta X_{growth}}{COD_{total} \times Q_{influent} - COD_{effluent, dissolved} \times Q_{effluent}} \times f_{COD/VSS} \quad Eq. \, 8$$

Where, Y_{obs} is the observed yield in g COD_{produced}/g COD_{removed}; $f_{COD/_{VSS}}$ is the conversion factor of VSS to COD obtained from experimental data.

2.6 Microbial community analysis

Sludge samples collected at the end of each phase were stored at -80°C for microbial analysis. DNA was extracted using FastDNATM SPIN Kit for Soil following the modified protocol by increasing the homogenization time to 60s. ³² The quantity and quality of extracted DNA was detected by 260 nm absorbance and 260/280nm absorbance ratio respectively using Nanodrop (Thermo Scientific, Massachusetts, USA). The V4 region of 16s rRNA genes were amplified using universal primer 515F (5'-GTGYCAGCMGCCGCGGTAA) and 806R (5'-GGACTACNVGGGTWTCTAAT) and sequenced on the high-throughput Illumina platform at Mr. DNA (Shallowater, TX). Sequences were processed using DATA2 algorithm on QIIME2. ³³ Taxonomy was assigned with 99% similarity using Silva 138 database. α-diversity was analyzed using core-metrics-phylogenetic method in the q2-diversity plugin. ³³ Pairwise Spearman's correlation of reactor performance and operation conditions was conducted in R (Version 3.6.3). The metagenome prediction was analyzed using PICRUSt2 based on Kyoto Encyclopedia of Genes and Genomes (KEGG) database. ^{34,35}

2.7 Statistical analysis

The Shapiro-Wilk test was used to test the normality of the data. Comparisons between several groups were performed using the parametric analysis of variance (ANOVA) test. Student's t-tests were used to test whether two sets of data are significantly different. For all tests, a significant level of 95% is applied. The statistical

analysis was conducted using SigmaPlot. The correlation between reactor performance and microbial communities was analyzed by Spearman's rank correlation analysis. Fruchterman-Reingold layout algorithm and Spearman's rank correlation analysis were used to plot the co-occurrence network.

3. Results and discussion

3.1 Reactor performance and the fate of COD

The overall COD removal efficiencies of HiCS ranged from 52.6% -74.5% for all six stages of operation (Fig. 2). When aeration was only provided in the stabilization phase (S-A), tCOD removal efficiencies decreased when SRT reduced from 3 days to 1.3 days and AerSRT reduced from 1 days to 0.43 days (Table 2). However, when aeration was provided in both contact and stabilization phases (C-S-A), decreasing SRT from 3 days to 1.3 days did not affect the tCOD removal efficiencies significantly. sCOD was the major composition in the effluent, accounting for 50.9%-82.1% of the total COD. The percentage of pCOD in the effluent decreased significantly with the increase of SRT under both aeration conditions (Table S4). pCOD in the effluent was reduced from 73±7 mg/L to 21±4 mg/L, and 84±5 mg/L to 23±5 mg/L under S-A and C-S-A conditions, respectively, when SRT increased from 1.3 days to 3 days. The increase of SRT improved the solubilization of organic matters, resulting in lower pCOD in the effluent.

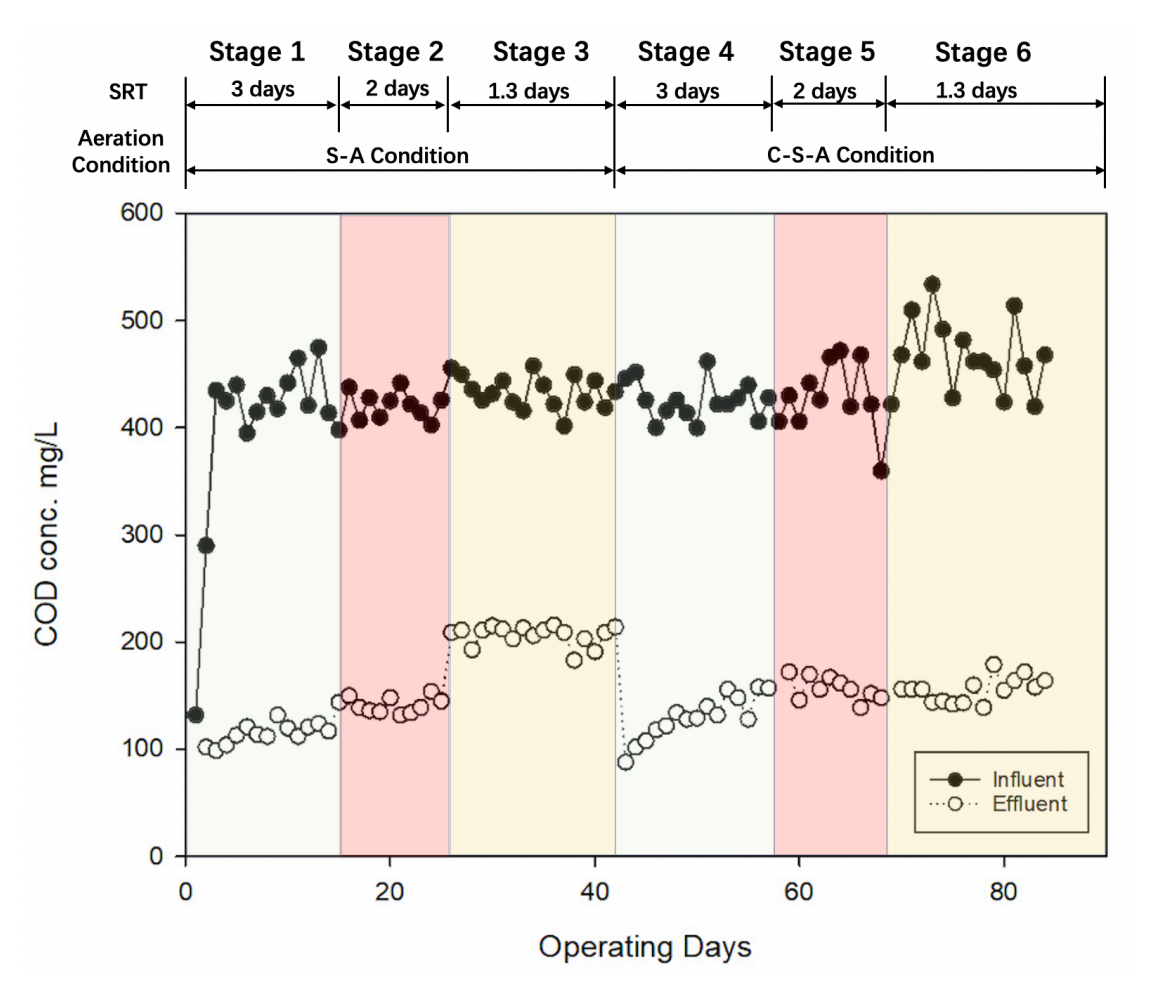


Fig. 2. Average COD concentrations of the two HiCS reactors at various operational conditions.

The carbon capture efficiency increased when SRT was reduced from 3 days to 1.3 days in both S-A and C-S-A conditions. At the lowest SRT, the highest carbon capture efficiencies achieved for S-A and C-S-A were 42.2% and 47.0%, respectively. The carbon oxidation efficiency showed reverse trends with carbon capture efficiency (Table 2). Similar results were reported that reduced SRT promoted carbon capture efficiency but negatively affected tCOD removal efficiency. ²⁴ The aeration condition affects the carbon capture efficiency significantly, and the addition of contact-phase aeration (C-S-A) yielded higher efficiencies in all SRTs (Table 2).

HiCS selected fast-growing microorganisms and the observed growth yields also

increased with the decrease of SRTs (Table 2). The sludge concentrations, as indicated by VSS, declined with decreasing SRT. The observed yields of sludge under C-A conditions increased from 0.44 to 0.70 gCOD_{sludge}·gCOD_{removed}⁻¹ with decreasing SRT from 3 days to 1.3 days. In the presence of contact-phase aeration (C-S-A), this effect was less pronounced, with observed yields increasing slightly from 0.58 to 0.69 gCOD_{sludge}·gCOD_{removed}⁻¹. Similar results were also observed in HRAS where observed yield increased from 0.33 to 0.53 gVSS·gCOD⁻¹ when SRT decreased from 2 to 0.3 days. ³⁶ The F/M ratio in the HiCS systems were 2.5 – 5.4 gCOD·gVSS⁻¹·d⁻¹, within the range of recommended F/M ratio of 2-10 gCOD·gVSS⁻¹·d⁻¹ for high-rate activated sludge systems. ³⁷ The high F/M ratio along with low SRT can select heterotrophic bacteria that can rapidly multiply and minimize biomass loss from endogenous decay, resulting in high observed yields. ³⁸ A positive correlation between the F/M ratio and specific COD removal rates was observed during the experiment (Table 2). For the S-A and C-S-A conditions, the peak specific COD removal rates are 6.47 and 7.42 g COD removed·gVSS⁻¹·d⁻¹, respectively, achieved at F/M ratios of 5.34 and 5.43 gCOD·gVSS⁻¹·d⁻¹. This trend is favorable for enhancing carbon capture efficiency in high-rate system. TN removal efficiencies were affected by both SRT and aeration conditions (Table 2). TN removal efficiencies decreased from 60.7% to 34.8% and from 43.7% to 19.0% under S-A and C-S-A conditions, respectively, when decreasing the SRTs from 3 days to 1.3 days. The sufficient carbon source combined with the longer anoxic condition in

the contact phase under S-A conditions may have promoted the denitrification and

270

271

272

273

274

275

276

277

278

279

280

281

282

283

284

285

286

287

288

289

290

resulted in higher TN removal efficiencies. Microbial analysis indicated that the relative abundance of *Nitrospira* was increased from 0.03% to 1.36% under S-A conditions and from 0.04% to 0.24% under C-S-A conditions when increasing SRT from 1.3 days to 3 days, respectively. Aeration under stabilization phase with SRT of 3 days had the highest relative abundance of *Nitrospira* and the highest TN removal efficiency.

The TP removal efficiencies under C-S-A conditions were generally higher than those under S-A conditions (Table 2). Under C-S-A conditions, TP removal decreased with decreasing SRT. Under S-A conditions, however, varying SRTs from 3 to 1.3 days had little impact on TP removal efficiencies (p = 0.075). The variation in TP removal efficiencies can be linked to the activity of polyphosphate-accumulating organisms (PAOs). According to PICRUSt2 metagenome prediction, the relative abundance of key enzyme (polyphosphate kinase, exopolyphosphatase, alkaline phosphatase) in PAOs was higher under C-S-A at 1.3 days SRT (Table S1), which also showed higher TP removal efficiencies than those of S-A conditions. Polyphosphate kinase and exopolyphosphatase are involved in the synthesis and degradation of polyphosphate, while alkaline phosphatase contributes to the hydrolysis of polyphosphate, transforming it into inorganic phosphorus in the biological phosphorus removal process.

309 39

TP removal may also be associated with the synthesis of PHA since with the assistance of exopolyphosphatase, PAOs can harness the energy yielded from polyphosphate degradation under anaerobic conditions to accumulate PHAs. In this research, the major composition of PHAs is PHB, thus those genes may be related with

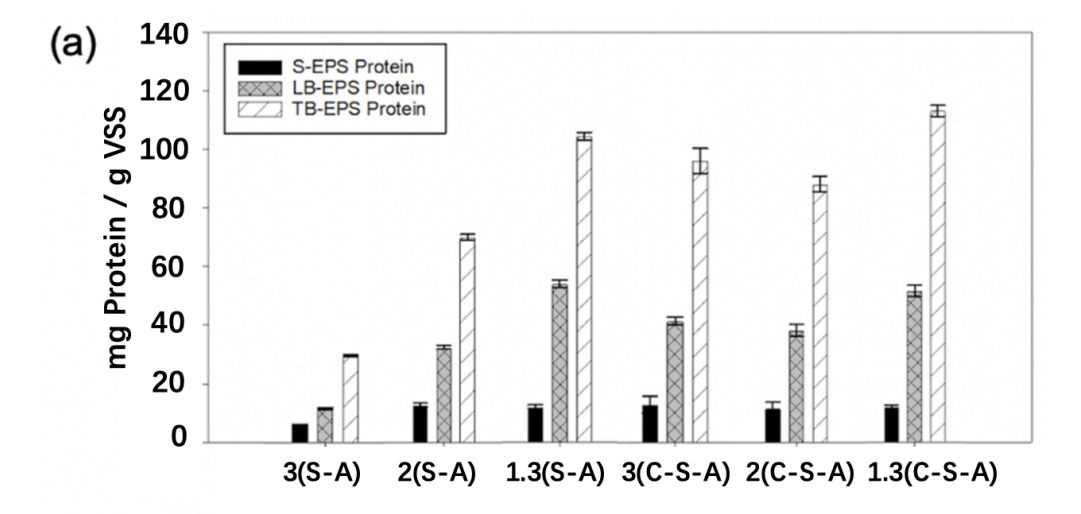
PHB production. Additionally, PAOs can also accumulate PHAs in the presence of excess of organic carbon under aerobic conditions. ⁴⁰ It is important to note that the synthetic wastewater used in this study contained acetate, a vital carbon source that is beneficial for PAOs. Further discussion will be presented in Section 3.3.

	Total SRT (d)	tCOD removal efficienc y (%)	COD oxidation efficiency (%)	COD capture efficiency (%)	TN removal efficiency (%)	TP removal efficiency (%)	Effluent tCOD/TN Ratio	$\begin{array}{c} Observed\ yield\\ (gCOD_{sludge}\cdot gC\\ OD_{removed}^{-1}) \end{array}$	$f_{\text{COD/VSS}} \ (g C O D_{\text{sludge}} \cdot g \ (V S S^{-1})$	F/M ratio (gCOD·gVSS ⁻¹ ·d ⁻¹)	Specific COD removal rates (g COD removed/g VSS/day)
Stabilizati	1.3	52.6±0.5	18.3	42.2	34.8±2.18	12.8±0.20	6.13	0.70	1.52	5.34	6.47
on- Aeration	2	65.6±0.8 2	33.4	34.9	39.1±2.63	17.6±0.03	5.5	0.58	1.49	4.11	5.62
(S-A)	3	72.6±0.6 9	37.2	36.9	60.7 ± 0.89	15.7±0.06	6.56	0.44	1.42	2.49	3.68
Contact-	1.3	63.2±0.3 9	20.8	47.0	19.0±1.73	25.0±0.84	3.75	0.69	1.72	5.43	7.41
Stabilizati on-	2	66.3±0.4 9	22.6	46.4	30.27±2.63	29.1±1.03	4	0.67	1.58	3.29	4.53
Aeration (C-S-A)	3	74.9±0.5 9	28.7	39.6	43.7±2.62	31.8±1.11	4.98	0.58	1.54	2.50	3.41

3.2 EPS production

EPS is important for the biosorption of organics from wastewater contributing to carbon capture. ⁴¹ The protein and polysaccharide contents in TB-EPS were always the highest among all types of EPS (Fig. 3). The protein concentrations in all EPS fractions were 3-6 times higher than the polysaccharide concentrations, which is similar to previous research on activated sludge. ²⁴ A positive relationship (R²=0.77) of the total EPS-protein and organic carbon capture efficiency was observed through Spearman's rank correlation analysis (Fig S1).

The protein and polysaccharide concentrations in all types of EPS (S-EPS, LB-EPS, and TB-EPS) increased with the decrease of SRTs (Fig. 3). The highest total EPS-protein concentrations at SRT of 1.3 days for S-A and C-S-A were 164 and 176 mg protein/g VSS, respectively. The total EPS-polysaccharide concentrations were 29.6 and 44.5 mg polysaccharide/g VSS at SRT of 1.3 days, respectively. C-S-A conditions showed higher total EPS production than that of S-A conditions.



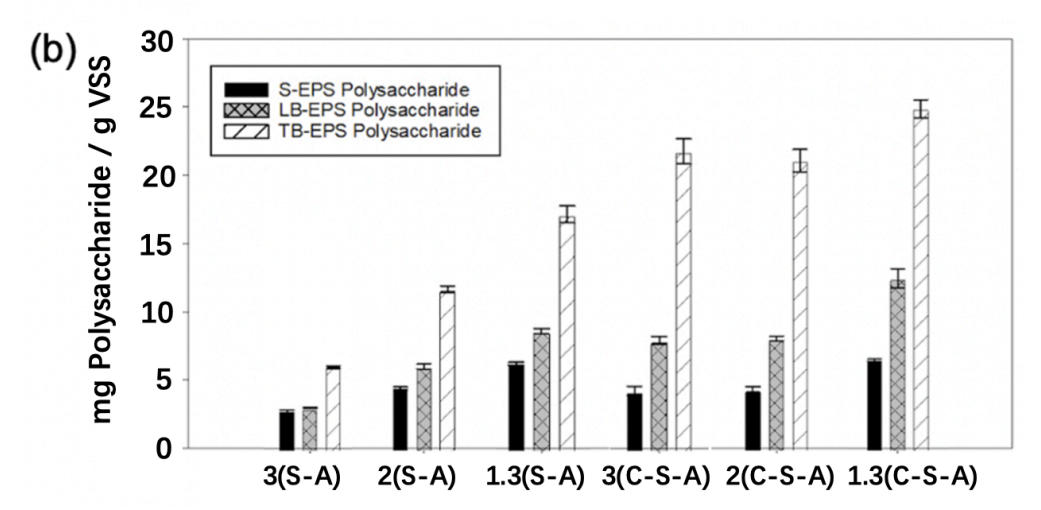


Fig. 3. EPS production. (a). EPS protein concentrations; (b). EPS polysaccharide concentrations. S-EPS: Soluble EPS; LB-EPS: Loosely-bound EPS; TB-EPS: Tightly-bound EPS.

3.3 PHA production

The PHA types measured in this study are PHB, PHV and PH2MV, while no PH2MV production was detected. The concentrations of PHB were 3 to 6 times greater than PHV in all HiCS stages (Fig. 4). The production of PHAs is affected by the carbon sources of the wastewater. Previous research showed that acetate primarily induces PHB production, while propionate leads to PHV production. ⁴² In this study, a considerable concentration of COD (176 mg/L) in the feedstock was attributed to

sodium acetate, leading to a higher content of PHB than that of PHV.

The production of PHB was also affected by SRT and aeration conditions. In general, PHB production increased with the decrease of SRT. C-S-A had significantly higher PHB production than that of S-A conditions at SRTs of 1.3 and 2 days (P<0.05). When feeding the reactor during the contact phase, microorganisms can use oxygen to provide required energy for the transmembrane transport of small molecular organic matters to synthesize storage compounds. ⁴³ While the lack of DO under S-A conditions in the contact phase resulted in insufficient ATP to synthesize PHA from acetate to acetyl-CoA. ⁴⁴ The results were also confirmed by PICRUSt2 function prediction that at 1.3 days SRT, the expression of key genes for PHA synthesis, 3-hydroxybutyryl-CoA dehydrogenase, acetyl-CoA acyltransferase, acetyl-CoA C-acetyltransferase and Poly (3-hydroxyalkanoate) polymerase (PhaC), was higher under C-S-A conditions than those under S-A conditions (Table S1).

Furthermore, the existence of the aerobic-anoxic cycle in S-A conditions led to more denitrification. The organic carbon would be consumed by the denitrification rather than absorbed or stored in the cell. While the higher AerSRT under C-S-A limited the carbon consumption by denitrification. Genes involved in PHB synthesis also showed negative correlation with key enzymes in PAO such as polyphosphate kinase and exopolyphosphatase, while demonstrating a positive correlation with alkaline phosphatase (Fig. S2). The results of gene prediction may represent the predominant mechanism governing phosphorus removal involving alkaline phosphatase.

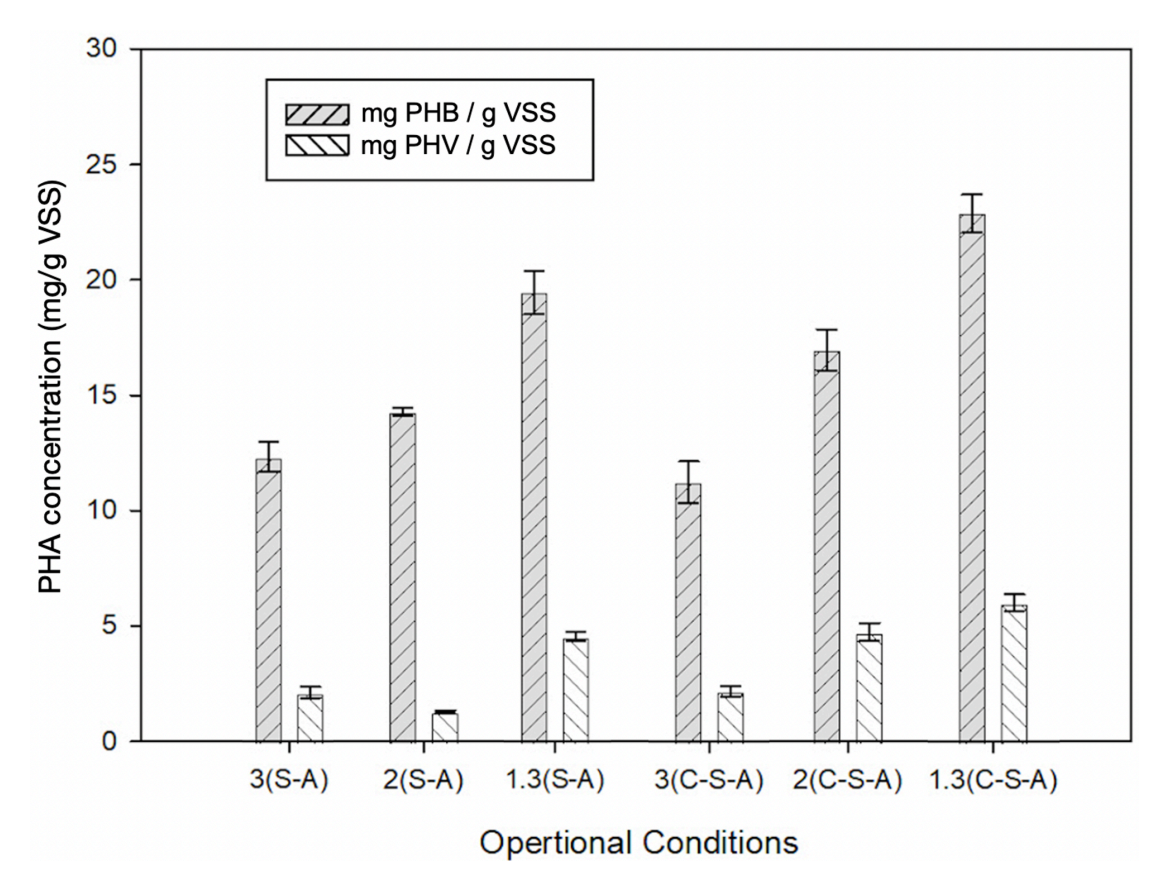


Fig 4. Polyhydroxalkanoates (PHA) content in the biomass. (PHB: polyhydroxybutyrate; PHV: polyhydroxyvalerate)

3.4 Microbial communities under various operational conditions

Microbial community composition was analyzed by high-throughput sequencing and the top 16 dominant microorganisms at genus level are shown in Fig. 5. A few genera, such as *Aquabacterium*, *Acinetobacter* and *Limnohabitans*, were abundant throughout all stages. Both the SRT and the aeration conditions affected the dominant genera of the HiCS reactors. Comparing S-A and C-S-A conditions, results showed that *Aquabacterium*, *Leptothrix* and *Limnohabitans* dominated in the more aerated C-S-A condition, while *Acinetobacter* was the dominant genus in the absence of contact-phase aeration (S-A condition). The abundance of *Aquabacterium* increased from 11.83% to 20.12% when shifting aeration from S-A to C-S-A at SRT of 1.3 days.

Reducing SRT from 3 to 1.3 days led to an increase of *Acinetobacter* from 18.68% to 26.73% under S-A condition, and from 0.84% to 3.98% under C-S-A condition. *Aquabacterium* was also increased from 2.64% to 11.83 % under S-A condition and from 4.77% to 20.12 % for C-S-A condition when reducing SRT from 3 days to 1.3 days. *Acinetobacter* includes anoxic heterotrophic bacteria which are related with enhanced biological phosphorus removal. ^{45,46} While *Aquabacterium* have the potential for denitrification and PHB synthesis. ^{47,48}

The decrease of SRT decreased the α-diversity of the microbial community (Table S2). Under the same SRT, S-A conditions yielded a higher Shannon's diversity index than C-S-A, probably due to the anoxic/anaerobic phases providing niches for more diverse microorganisms, while the contact-phase aeration induced an aerobic environment for most of the time (C-S-A). With the decrease of SRT (from 3 days to 1.3 days), the Ace and Chao1 indices of the samples were found to decrease as well, indicating a greater richness of the microbial community at longer SRT.

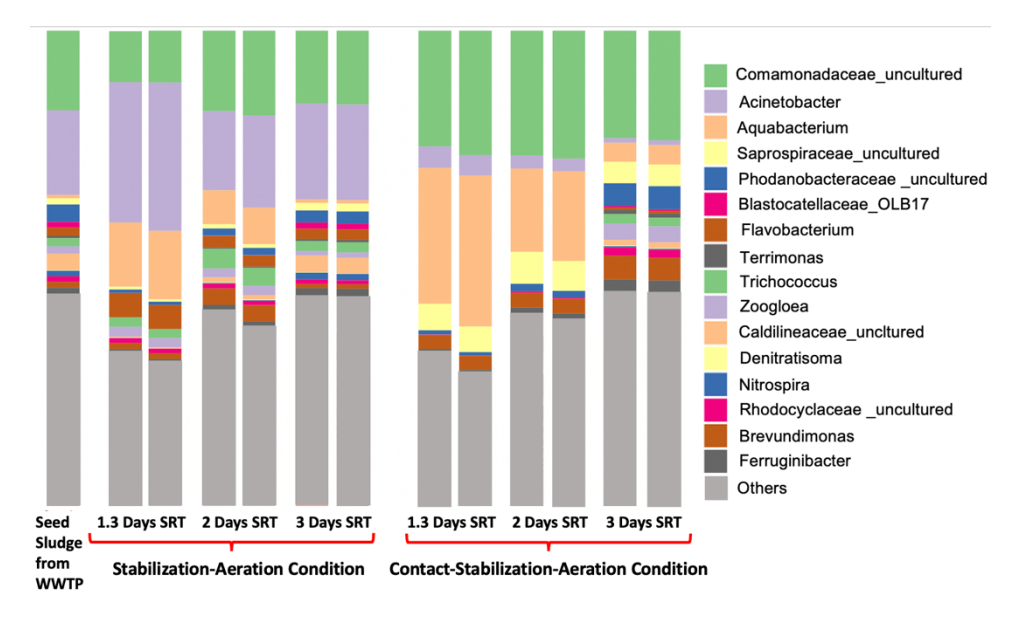


Fig. 5. Microbial community composition at the genus level as determined by 16S RNA

sequencing of sludge from the HiCS reactors. (Color labels in the figure are arranged from top to bottom)

3.5 Operational conditions induced changes of microbial community and reactor

performance

The trade-off between tCOD removal and carbon capture efficiency observed in our study underscores the complexity of optimizing reactor performance. The production of EPS and PHA showed a positive correlation with organic carbon capture efficiency which is consistent with previous research. 24 In the HiCS system, changing operational conditions affected the microbial communities: SRT had a greater impact on α -diversity and richness, whereas the aeration condition, or the ratio of aeration to anoxic/anaerobic time, influenced the dominant genera. Ultimately, these shifts in the microbial community result in changes to HiCS reactor performance, such as EPS and PHA production, tCOD removal, and carbon capture efficiency.

The co-occurrence networks and correlation analysis further reveal the complex relationships within microbial genera and their connections to system performance metrics. The co-occurrence networks of microbial genus were divided into five clusters (Fig. 6a). Each cluster represents closely connected genera which showed similar trends in the correlation analysis (Fig. 6b). Certain genera like *Aquabacterium* and *Leptothrix* were positively correlated with organic carbon capture efficiency and EPS production but negatively correlated with COD oxidation, presumably indicating their role in organic carbon capture. This suggests that genera with similar functions may prefer specific operational conditions. The dominant genera under S-A conditions showed no

correlation with EPS production, whereas under C-S-A conditions, dominant genera like Aquabacterium (20% of bacterial community) and Leptothrix (9.1% of the community) were positively correlated with EPS production, where higher carbon capture efficiencies were also observed. The dominant genera under S-A conditions, Acinetobacter and Limnohabitans (Fig. 6a, blue cluster), showed no correlation with EPS production and observed yields. These findings highlight the importance of understanding the environmental factors that shape microbial communities in the HiCS reactor, which can inform strategies for optimizing reactor performance. Previous research has observed the applicability of traditional niche theory in activated sludge ecosystems, which are highly managed systems. ⁴⁹ Griffin and Wells proposed that there is strong synchronicity in community composition between reactors of different scales under identical seasonal and temperature conditions. ⁵⁰ Whether similar community structures are found in HiCS reactors of varying scales under the same operational conditions warrants further investigation. More profound understanding of the impact of shifts in microbial communities on reactor performance is needed to enhance the carbon capture efficiencies in HiCS systems.

418

419

420

421

422

423

424

425

426

427

428

429

430

431

432

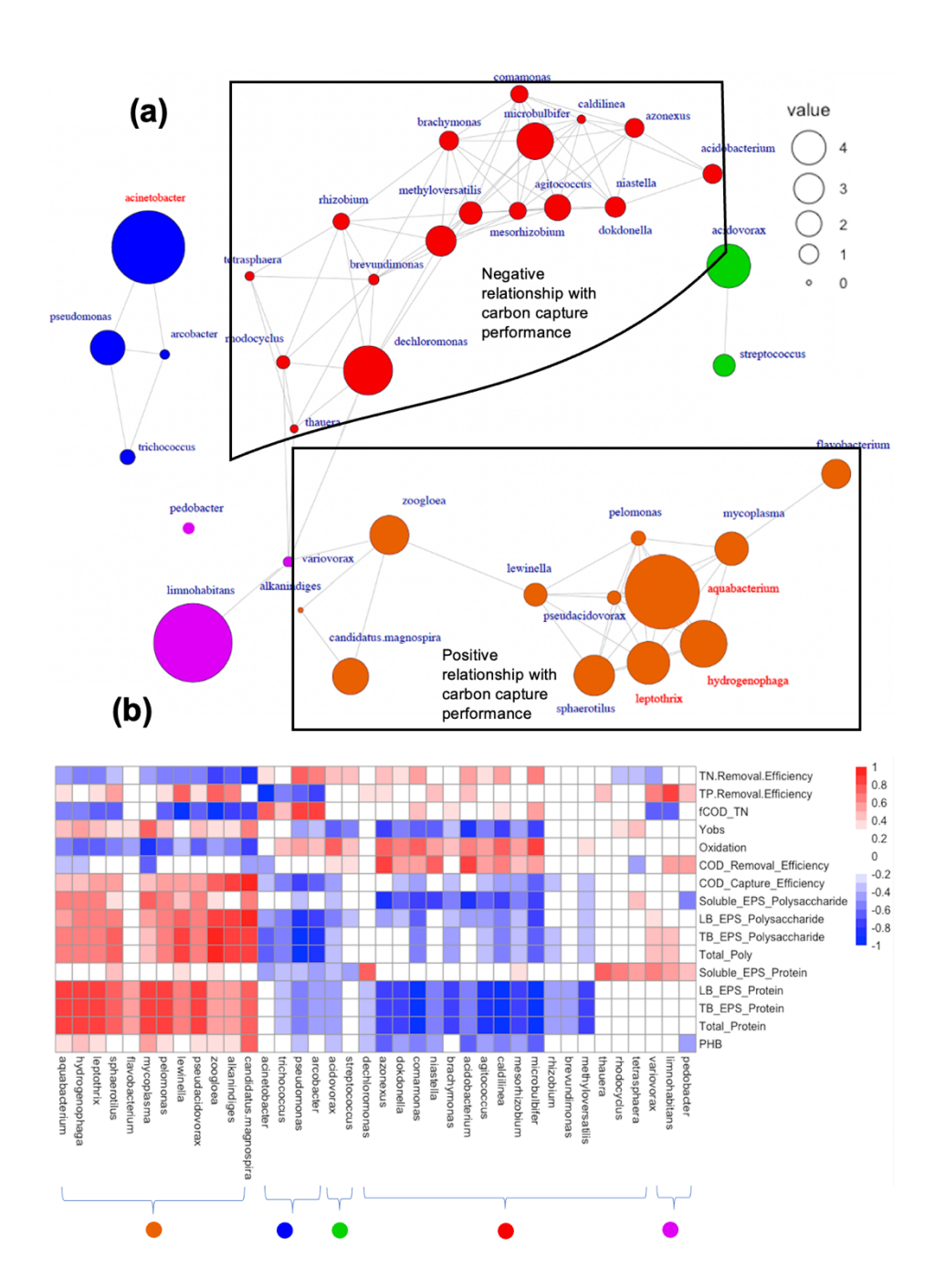


Fig. 6. (a). The 37 most abundant genera and positive co-occurrence networks in the HiCS microbial communities (color represents clustered groups); (b). Correlation

between microbial genus and reactor performance.

439

440

441

442

443

444

445

446

447

448

449

450

451

452

453

454

455

456

457

438

4. Conclusions

This research on the HiCS process demonstrated dynamic interactions between microbial communities and operational parameters, particularly SRT and aeration modes. A shift in these parameters resulted in significant changes in the composition and diversity of microbial communities and, subsequently, in the HiCS reactor performance. An SRT of 1.3 days with aeration under both contact and stabilization phases yielded the highest carbon capture efficiency. PHB was the major PHA product under all the operational conditions. High-throughput sequencing revealed that Aquabacterium was the dominant genus under C-S-A conditions, while Acinetobacter was dominant under S-A conditions. The decrease of SRT from 3 days to 1.3 days led to an increase of the relative abundances of Aquabacterium and Acinetobacter under both C-S-A and S-A conditions. The co-occurrence and correlation analysis indicated that genera such as Aquabacterium and Leptothrix were positively correlated with carbon capture efficiency and EPS production, while negatively correlated with carbon oxidation. Our findings highlight the necessity of understanding these interplays for effective optimization of HiCS reactor performance. Future research should focus on how changes in microbial communities under different operational conditions influence the reactor performance when scaling up.

458

459

5. Acknowledgements

- This material is based upon work supported by the US National Science
- 461 Foundation under Grant No.2000761 and Wastewater Management Grant from the
- Office of Physical Plant at The Pennsylvania State University. Any opinions, findings,
- and conclusions or recommendations expressed in this material are those of the authors
- and do not necessarily reflect the views of the sponsors.

- Supporting Information: The additional information details about microbial analysis
- 467 (PICRUSt2 metagenome prediction, α-diversity and correlation analysis) and
- characteristics of synthetic wastewater, real wastewater and effluent.

- 470 References
- 471 (1) Pabi, S.; Amarnath, A.; Goldstein, R.; Reekie, L. Electricity Use and
- 472 Management in the Municipal Water Supply and Wastewater Industries. *Electric*
- 473 Power Research Institute, 2013, 194.
- 474 (2) Gude, V. G. Energy and Water Autarky of Wastewater Treatment and Power
- Generation Systems. *Renewable and sustainable energy reviews* **2015**, *45*, 52–68.
- 476 (3) Wan, J.; Gu, J.; Zhao, Q.; Liu, Y. COD Capture: A Feasible Option towards
- Energy Self-Sufficient Domestic Wastewater Treatment. Scientific reports 2016, 6
- 478 (1), 1–9.
- 479 (4) Rahman, A.; Meerburg, F. A.; Ravadagundhi, S.; Wett, B.; Jimenez, J.; Bott, C.;
- 480 Al-Omari, A.; Riffat, R.; Murthy, S.; De Clippeleir, H. Bioflocculation Management
- 481 through High-Rate Contact-Stabilization: A Promising Technology to Recover
- Organic Carbon from Low-Strength Wastewater. Water Research 2016, 104, 485–
- 483 496.
- 484 (5) Marani, D.; Renzi, V.; Ramadori, R.; Braguglia, C. Size Fractionation of COD in
- 485 Urban Wastewater from a Combined Sewer System. Water Science and Technology
- 486 **2004**, *50* (12), 79–86.
- 487 (6) Rahman, A.; Hasan, M.; Meerburg, F.; Jimenez, J. A.; Miller, M. W.; Bott, C. B.;
- 488 Al-Omari, A.; Murthy, S.; Shaw, A.; De Clippeleir, H.; Riffat, R. Moving Forward
- with A-Stage and High-Rate Contact-Stabilization for Energy Efficient Water
- 490 Resource Recovery Facility: Mechanisms, Factors, Practical Approach, and
- 491 Guidelines. *Journal of Water Process Engineering* **2020**, *36*, 101329.
- 492 https://doi.org/10.1016/j.jwpe.2020.101329.

- 493 (7) Cagnetta, C.; Saerens, B.; Meerburg, F. A.; Decru, S. O.; Broeders, E.; Menkveld,
- 494 W.; Vandekerckhove, T. G.; De Vrieze, J.; Vlaeminck, S. E.; Verliefde, A. R. High-
- 495 Rate Activated Sludge Systems Combined with Dissolved Air Flotation Enable
- 496 Effective Organics Removal and Recovery. Bioresource technology 2019, 291,
- 497 121833.
- 498 (8) Jimenez, J. A.; La Motta, E. J.; Parker, D. S. Kinetics of Removal of Particulate
- 499 Chemical Oxygen Demand in the Activated-Sludge Process. Water Environment
- 500 Research **2005**, 77 (5), 437–446.
- 501 (9) Garikipati, S. Evaluation of Colloidal Titration for the Determination of Surface
- 502 Charge of Activated Sludge Flocs, Master's Thesis. Chalmers University of
- 503 Technology. Sweden, 2005.
- 504 (10) Fernández, I.; Dosta, J.; Fajardo, C.; Campos, J.; Mosquera-Corral, A.; Méndez,
- 505 R. Short-and Long-Term Effects of Ammonium and Nitrite on the Anammox Process.
- *Journal of Environmental Management* **2012**, *95*, S170–S174.
- 507 (11) Van Loosdrecht, M.; Pot, M.; Heijnen, J. Importance of Bacterial Storage
- Polymers in Bioprocesses. Water Science and Technology 1997, 35 (1), 41–47.
- 509 (12) Wang, H.; Wang, S.-X.; Ren, Z.-Q.; Chen, S.-N.; Liu, M.; Huang, B.-C.; Jin, R.-
- 510 C. Performance and Mechanism of Improved Soluble Organic Carbon Recovery from
- Municipal Wastewater through the Coagulation-Enhanced High-Rate Contact
- 512 Stabilization Process. *ACS EST Eng.* **2023**, *3* (2), 174–182.
- 513 https://doi.org/10.1021/acsestengg.2c00268.
- 514 (13) Liang, M.; Lu, X.; Liu, P.; Wu, X.; Zan, F. Tapping the Energy Potential from
- Wastewater by Integrating High-Rate Activated Sludge Process with Anaerobic
- Membrane Bioreactor. *Journal of Cleaner Production* **2022**, *333*, 130071.
- 517 https://doi.org/10.1016/j.jclepro.2021.130071.
- 518 (14) Ngo, K. N.; Tampon, P.; Van Winckel, T.; Massoudieh, A.; Sturm, B.; Bott, C.;
- Wett, B.; Murthy, S.; Vlaeminck, S. E.; DeBarbadillo, C.; De Clippeleir, H.
- 520 Introducing Bioflocculation Boundaries in Process Control to Enhance Effluent
- Quality of High-Rate Contact-Stabilization Systems. Water Environment Research
- 522 **2022**, *94* (8), e10772. https://doi.org/10.1002/wer.10772.
- 523 (15) Kinyua, M. N.; Miller, M. W.; Wett, B.; Murthy, S.; Chandran, K.; Bott, C. B.
- Polyhydroxyalkanoates, Triacylglycerides and Glycogen in a High Rate Activated
- 525 Sludge A-Stage System. *Chemical Engineering Journal* **2017**, *316*, 350–360.
- 526 (16) Bhatia, S. K.; Otari, S. V.; Jeon, J.-M.; Gurav, R.; Choi, Y.-K.; Bhatia, R. K.;
- Pugazhendhi, A.; Kumar, V.; Banu, J. R.; Yoon, J.-J. Biowaste-to-Bioplastic
- 528 (Polyhydroxyalkanoates): Conversion Technologies, Strategies, Challenges, and
- Perspective. *Bioresource Technology* **2021**, *326*, 124733.
- 530 (17) Faust, L.; Temmink, H.; Zwijnenburg, A.; Kemperman, A. J.; Rijnaarts, H. Effect
- of Dissolved Oxygen Concentration on the Bioflocculation Process in High Loaded
- 532 MBRs. Water research **2014**, 66, 199–207.
- 533 (18) Dolejs, P.; Gotvald, R.; Velazquez, A. M.; Hejnic, J.; Jenicek, P.; Bartacek, J.
- Contact Stabilization with Enhanced Accumulation Process for Energy Recovery
- from Sewage. *Environmental Engineering Science* **2016**, *33* (11), 873–881.
- 536 (19) Dai, W.; Xu, X.; Yang, F. High-Rate Contact Stabilization Process-Coupled

- 537 Membrane Bioreactor for Maximal Recovery of Organics from Municipal
- 538 Wastewater. Water **2018**, 10 (7), 878.
- 539 (20) Chase, J. M.; Leibold, M. A. Ecological Niches: Linking Classical and
- 540 Contemporary Approaches; University of Chicago Press, 2009.
- 541 (21) Ishii, S.; Suzuki, S.; Norden-Krichmar, T. M.; Wu, A.; Yamanaka, Y.; Nealson,
- 542 K. H.; Bretschger, O. Identifying the Microbial Communities and Operational
- 543 Conditions for Optimized Wastewater Treatment in Microbial Fuel Cells. Water
- 544 research **2013**, 47 (19), 7120–7130.
- 545 (22) Yang, B.; Wang, J.; Wang, J.; Xu, H.; Song, X.; Wang, Y.; Li, F.; Liu, Y.; Bai, J.
- 546 Correlating Microbial Community Structure with Operational Conditions in
- 547 Biological Aerated Filter Reactor for Efficient Nitrogen Removal of Municipal
- 548 Wastewater. *Bioresource technology* **2018**, *250*, 374–381.
- 549 (23) Rahman, A.; De Clippeleir, H.; Thomas, W.; Jimenez, J. A.; Wett, B.; Al-Omari,
- A.; Murthy, S.; Riffat, R.; Bott, C. A-Stage and High-Rate Contact-Stabilization
- Performance Comparison for Carbon and Nutrient Redirection from High-Strength
- Municipal Wastewater. *Chemical Engineering Journal* **2019**, *357*, 737–749.
- 553 (24) Meerburg, F. A.; Boon, N.; Van Winckel, T.; Pauwels, K. T. G.; Vlaeminck, S. E.
- Live Fast, Die Young: Optimizing Retention Times in High-Rate Contact
- 555 Stabilization for Maximal Recovery of Organics from Wastewater. *Environ. Sci.*
- 556 *Technol.* **2016**, *50* (17), 9781–9790. https://doi.org/10.1021/acs.est.6b01888.
- 557 (25) Aiyuk, S.; Verstraete, W. Sedimentological Evolution in an UASB Treating
- 558 SYNTHES, a New Representative Synthetic Sewage, at Low Loading Rates.
- 559 *Bioresource Technology* **2004**, *93* (3), 269–278.
- 560 (26) Coma, M.; Puig, S.; Monclús, H.; Balaguer, M.; Colprim, J. Effect of Cycle
- 561 Changes on Simultaneous Biological Nutrient Removal in a Sequencing Batch
- 562 Reactor (SBR). *Environmental technology* **2010**, *31* (3), 285–294.
- 563 (27)Li, X. Y.; Yang, S. F. Influence of Loosely Bound Extracellular Polymeric
- 564 Substances (EPS) on the Flocculation, Sedimentation and Dewaterability of Activated
- 565 Sludge. *Water Research* **2007**, *41* (5), 1022–1030.
- 566 https://doi.org/10.1016/j.watres.2006.06.037.
- 567 (28) Lowry, O. H. Protein Measurement with the Folin Phenol Reagent. J biol Chem
- 568 **1951**, *193*, 265–275.
- 569 (29) Dubois, M.; Gilles, K. A.; Hamilton, J. K.; Rebers, P. t; Smith, F. Colorimetric
- 570 Method for Determination of Sugars and Related Substances. *Analytical chemistry*
- 571 **1956**, *28* (3), 350–356.
- 572 (30) APHA. Standard Methods for the Examination of Water and Wastewaters (23rd,
- 673 ed). American Public Health Association, American Water Works Association, Water
- 574 Environment Federation, **2017**.
- 575 (31) Meerburg, F. A.; Boon, N.; Van Winckel, T.; Vercamer, J. A. R.; Nopens, I.;
- Vlaeminck, S. E. Toward Energy-Neutral Wastewater Treatment: A High-Rate
- 577 Contact Stabilization Process to Maximally Recover Sewage Organics. *Bioresource*
- 578 *Technology* **2015**, *179*, 373–381. https://doi.org/10.1016/j.biortech.2014.12.018.
- 579 (32) Agrawal, S.; Weissbrodt, D. G.; Annavajhala, M.; Jensen, M. M.; Arroyo, J. M.
- 580 C.; Wells, G.; Chandran, K.; Vlaeminck, S. E.; Terada, A.; Smets, B. F.; Lackner, S.

- Time to Act–Assessing Variations in qPCR Analyses in Biological Nitrogen Removal
- with Examples from Partial Nitritation/Anammox Systems. Water Research 2021,
- 583 *190*, 116604. https://doi.org/10.1016/j.watres.2020.116604.
- 584 (33) Bolyen, E.; Rideout, J. R.; Dillon, M. R.; Bokulich, N. A.; Abnet, C. C.; Al-
- 585 Ghalith, G. A.; Alexander, H.; Alm, E. J.; Arumugam, M.; Asnicar, F. Reproducible,
- Interactive, Scalable and Extensible Microbiome Data Science Using QIIME 2.
- 587 *Nature biotechnology* **2019**, *37* (8), 852–857.
- 588 (34) Douglas, G. M.; Maffei, V. J.; Zaneveld, J.; etc. PICRUSt2: An Improved and
- Customizable Approach for Metagenome Inference. *BioRxiv* **2020**, 672295. doi:
- 590 https://doi.org/10.1101/672295 (Accessed 08/23/2023)
- 591 (35)Louca, S.; Parfrey, L. W.; Doebeli, M. Decoupling Function and Taxonomy in
- the Global Ocean Microbiome. *Science* **2016**, *353* (6305), 1272–1277.
- 593 (36) Jimenez, J.; Miller, M.; Bott, C.; Murthy, S.; De Clippeleir, H.; Wett, B. High-
- 594 Rate Activated Sludge System for Carbon Management Evaluation of Crucial
- 595 Process Mechanisms and Design Parameters. *Water Research* **2015**, 87, 476–482.
- 596 https://doi.org/10.1016/j.watres.2015.07.032.
- 597 (37) Sancho, I.; Lopez-Palau, S.; Arespacochaga, N.; Cortina, J. L. New Concepts on
- 598 Carbon Redirection in Wastewater Treatment Plants: A Review. Science of The Total
- *Environment* **2019**, *647*, 1373–1384. https://doi.org/10.1016/j.scitotenv.2018.08.070.
- 600 (38) Metcalf, L. Wastewater Engineering: Treatment and Reuse. Metcalf & Eddy Inc.
- 601 **2003**.
- 602 (39) Kulakovskaya, T. V.; Vagabov, V. M.; Kulaev, I. S. Inorganic Polyphosphate in
- Industry, Agriculture and Medicine: Modern State and Outlook. *Process Biochemistry*
- 604 **2012**, *47* (1), 1–10.
- 605 (40) Ahn, J.; Schroeder, S.; Beer, M.; McIlroy, S.; Bayly, R. C.; May, J. W.;
- Vasiliadis, G.; Seviour, R. J. Ecology of the Microbial Community Removing
- 607 Phosphate from Wastewater under Continuously Aerobic Conditions in a Sequencing
- Batch Reactor. Applied and Environmental Microbiology 2007, 73 (7), 2257–2270.
- 609 (41) Huang, L.; Jin, Y.; Zhou, D.; Liu, L.; Huang, S.; Zhao, Y.; Chen, Y. A Review of
- 610 the Role of Extracellular Polymeric Substances (EPS) in Wastewater Treatment
- 611 Systems. International journal of environmental research and public health 2022, 19
- 612 (19), 12191.
- 613 (42) Jiang, Y.; Hebly, M.; Kleerebezem, R.; Muyzer, G.; van Loosdrecht, M. C. M.
- Metabolic Modeling of Mixed Substrate Uptake for Polyhydroxyalkanoate (PHA)
- 615 Production. *Water Research* **2011**, *45* (3), 1309–1321.
- 616 https://doi.org/10.1016/j.watres.2010.10.009.
- 617 (43) Anderson, A. J.; Dawes, E. Occurrence, Metabolism, Metabolic Role, and
- 618 Industrial Uses of Bacterial Polyhydroxyalkanoates. *Microbiological reviews* **1990**,
- 619 *54* (4), 450–472.
- 620 (44)Sun, S.; Ding, Y.; Liu, M.; Xian, M.; Zhao, G. Comparison of Glucose, Acetate
- and Ethanol as Carbon Resource for Production of Poly(3-Hydroxybutyrate) and
- 622 Other Acetyl-CoA Derivatives. Frontiers in Bioengineering and Biotechnology 2020,
- 623 8.
- 624 (45) Abdel-El-Haleem, D. Acinetobacter: Environmental and Biotechnological

- 625 Applications. *African Journal of Biotechnology* **2003**, *2* (4), 71–74.
- 626 https://doi.org/10.4314/ajb.v2i4.14828.
- 627 (46) Roguet, A.; Newton, R. J.; Eren, A. M.; McLellan, S. L. Guts of the Urban
- 628 Ecosystem: Microbial Ecology of Sewer Infrastructure. mSystems 2022, 7 (4),
- 629 e00118-22. https://doi.org/10.1128/msystems.00118-22.
- 630 (47) Feng, L.; Yan, J.; Jiang, Z.; Chen, X.; Li, Z.; Liu, J.; Qian, X.; Liu, Z.; Liu, G.;
- 631 Liu, C. Characterization of Polyhydroxybutyrate (PHB) Synthesized by Newly
- 632 Isolated Rare Actinomycetes Aquabacterium Sp. A7-Y. International Journal of
- 633 *Biological Macromolecules* **2023**, *232*, 123366.
- 634 (48)Lin, M.-C.; Jiang, S.-R.; Chou, J.-H.; Arun, A.; Young, C.-C.; Chen, W.-M.
- 635 Aquabacterium Fontiphilum Sp. Nov., Isolated from Spring Water. International
- *journal of systematic and evolutionary microbiology* **2009**, *59* (4), 681–685.
- 637 (49)Guo, B.; Manchester, M.; Luby, T.; Frigon, D. Composition of Heterotrophic
- 638 Specialized Sub-Guilds Defined by a Positive RNA and Polyhydroxyalkanoate
- 639 Correlation in Activated Sludge. *Water Research* **2018**, *144*, 561–571.
- 640 https://doi.org/10.1016/j.watres.2018.07.059.
- 641 (50) Griffin, J. S.; Wells, G. F. Regional Synchrony in Full-Scale Activated Sludge
- Bioreactors Due to Deterministic Microbial Community Assembly. *The ISME journal*
- 643 **2017**, *11* (2), 500–511.